

# FEASIBILITY STUDY OF A 1-MW PULSED SPALLATION SOURCE\*

Y. Cho, Y.-C. Chae, E. Crosbie, M. Fathizadeh, H. Friedsam, K. Harkay, D. Horan, S. Kim, R. Kustom, E. Lessner, W. McDowell, D. McGhee, F. Mills, H. Moe, R. Nielsen, G. Norek, K. J. Peterson, A. Rauchas, K. Symon, K. Thompson, D. Warner and M. White,  
Argonne National Laboratory, Argonne, IL 60439, USA.

## Abstract

A feasibility study of a 1-MW pulsed spallation source based on a rapidly cycling proton synchrotron (RCS) has been completed. The facility consists of a 400-MeV H<sup>+</sup> linac, a 30-Hz RCS that accelerates the 400-MeV beam to 2 GeV, and two neutron-generating target stations. The design time-averaged current of the accelerator system is 0.5 mA, and is equivalent to  $1.04 \times 10^{14}$  protons per pulse. The linac system consists of an H<sup>+</sup> ion source, a 2-MeV RFQ, a 70-MeV DTL and a 330-MeV CCL. Transverse phase space painting to achieve a Kapchinskij-Vladimirskij (K-V) distribution of the injected particles is accomplished by the charge exchange injection and programming of the closed orbit during the injection. The synchrotron lattice uses FODO cells of 90° phase advance. Dispersion-free straight sections are obtained by using a missing magnet scheme. Synchrotron magnets are powered by a dual-frequency resonance circuit that excites the magnets at a 20-Hz rate and de-excites them at a 60-Hz rate, resulting an effective rate of 30 Hz, and reducing the required rf power by 1/3. Details of the study are presented.

## I. INTRODUCTION

A proton synchrotron system capable of delivering 1 MW of beam power was designed for the Intense Pulsed Neutron Source (IPNS) Upgrade Feasibility Study at Argonne National Laboratory (ANL) [1]. The RCS and associated research facilities are housed in the 50,000 m<sup>2</sup> of space in the former 12-GeV Zero Gradient Synchrotron (ZGS) area. The ZGS Ring Building houses a 190-m circumference, 2-GeV RCS. Two adjoining experiment halls house two neutron generating target stations, each serving 18 neutron beamlines and instruments. Figure 1 shows the proposed facility layout. Enclosures for the linac and low energy transport line (LET) are the only new conventional facility construction, and are also shown in Figure 1. The choice of 30 Hz as the repetition rate of the fast cycling synchrotron was based on preferences expressed by the users.

## II. LATTICE

Required features of the lattice are: 1) To have a large transition energy so that the lattice has a relatively large slip factor,  $\eta = |\gamma^{-2} - \gamma_t^{-2}|$ , 2) to have enough straight section length for a radio-frequency cavity system that could have a total length of 20-30 m, and 3) the straight sections should be dispersion-free for implementation of charge-exchange

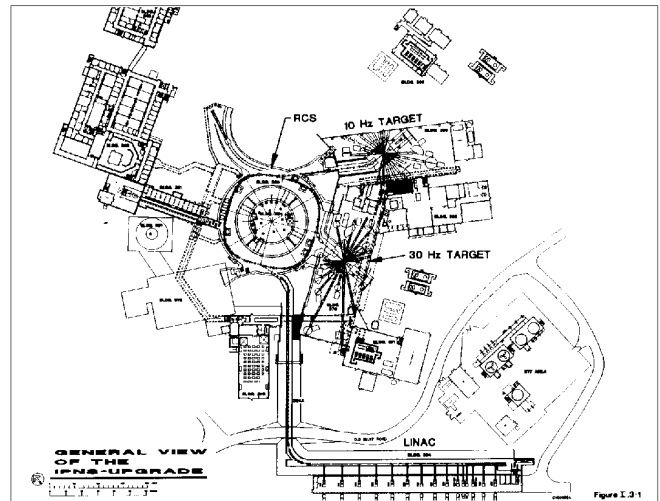


Figure 1: IPNS Upgrade Facility Layout.

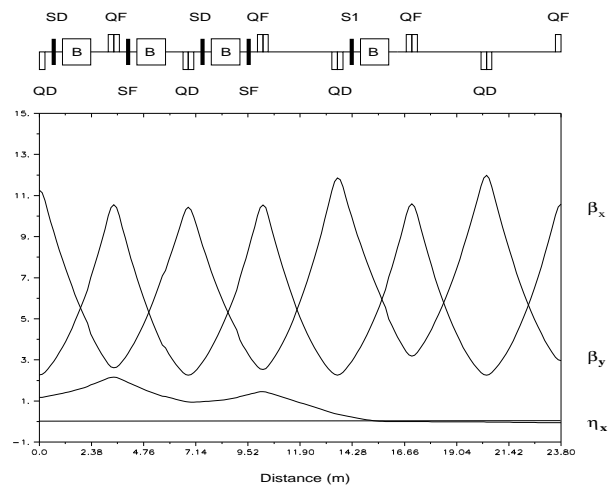


Figure 2: Lattice Functions for 1/2 Superperiod.

injection. Figure 2 shows 1/2 of a super period that has a reflective symmetry at both ends. Each cell of the FODO structure has a phase advance of  $\sim 90^\circ$  in both transverse planes. The normal cells, dispersion suppressor cell and the straight section cells are indicated in the figure. The dispersion suppressor cell is made by removing a dipole from a  $90^\circ$  phase advance cell. When the vertical phase advance is slightly less than  $90^\circ$  but the horizontal phase advance is maintained at  $90^\circ$ , the missing dipole scheme suppresses the dispersion function. An advantage of this arrangement is that when the total lattice is put together, the horizontal tune is about one unit higher than the vertical. The dynamic aperture study took alignment and

\* Work supported by the U. S. Department of Energy, Office of Basic Sciences under the Contract W-31-109-ENG-38.

construction imperfections into account, and the results are presented elsewhere [2]. Table 1 shows parameters of the normal cell.

Table 1 Normal Cell Parameters  
(2.2 GeV,  $B\rho = 9.989 \text{ Tm}$ )

Elements	Length (m)	Strength	Units
QD	0.25	-7.276	T/m
D1	0.3		
SD	0.2	-0.843	$\text{m}^{-2}$
D1	0.3		
B	1.3	1.5088	T
D2	0.8		
QF	0.5	8.267	T/m
D1	0.3		
SF	0.2	0.612	$\text{m}^{-2}$
D1	0.3		
B	1.3	1.5088	T
D2	0.8		
QD	0.25	-7.276	T/m

### III. INJECTION

The injection energy was determined by the incoherent space charge limit of the lattice and the defined acceptance of the synchrotron. If the injected beam stack has an emittance of  $375 \pi \text{ mm mrad}$  in both transverse planes, and the allowed tune shift due to space charge is 0.15, an injection energy of 400 MeV is sufficient to allow a time averaged current of 0.5 mA with a repetition rate of 30 Hz.

The 400-MeV  $\text{H}^-$  ion injector linac design for this feasibility study was performed by the industrial firm, AccSys Technology, Inc. The linac design specification includes: 1) an rms normalized emittance of  $1\pi \text{ mm mrad}$ , 2) an energy spread of less than 2.5 MeV, 3) a beam pulse length of 0.5 msec, and 4) beam chopping capability near the ion source so that the beam can be injected into a waiting synchrotron bucket.

Phase space painting in both transverse planes is used to stack 560 turns in the synchrotron. Four bumper magnets provide radial closed orbit displacement, and both injection position and angle can be radially adjusted as shown in Figure 3. A fast vertical steering magnet allows adjustment of the vertical injection angle. Unique features of this injection system include: 1) Trajectories of incoming  $\text{H}^-$  ions and of the circulating protons are combined by one of the ring focusing quadrupole magnets rather than by the customary dipole magnets. The use of this quadrupole has an added advantage in that the ring focusing quadrupole acts as a defocusing quadrupole for the incoming  $\text{H}^-$  beam, and it provides an additional bend for the  $\text{H}^-$  particles. There is ample separation between the incoming beam and the circulating beam. 2) Since each cell has  $90^\circ$  phase advance the bumper magnets, B1 and B4, shown in Figure 3, can displace and restore the closed orbit. However, B2 and B3 are needed to adjust the injection angle of the  $\text{H}^-$  ions so that  $\text{H}^0$  particles emerging from the stripping foil can be collected in a catcher. A discussion of the  $\text{H}^-$  and  $\text{H}^0$  particles associated with this injection system is given in reference [3].

Using the bumper system together with the vertical steering magnet in the transport line, the injected beam can be stacked in a K-V distribution [4].

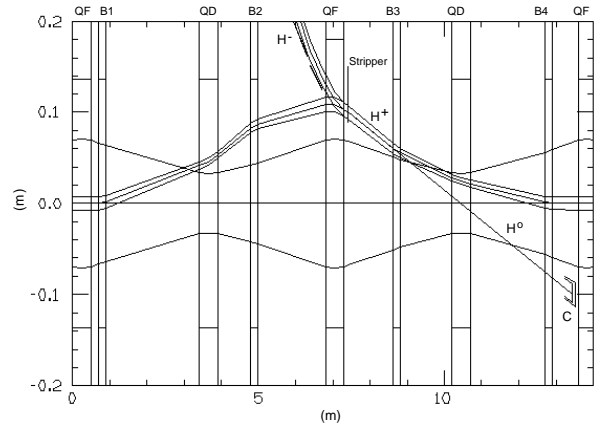


Figure 3: Bumped Orbit Injection, Showing the  $\text{H}^0$  Catcher.

### IV. RF VOLTAGE PROGRAM

A key goal of the design study was to devise an rf program that prevents beam loss from injection through acceleration to extraction. The rf program was obtained using a Monte Carlo program that tracked the particles from injection to extraction. The tracking study also provided information on optimum chopping of the incoming beam. In the context of bunch rotation, chopping is related to the energy spread of injected beam. Figure 4 shows the rf voltage program and the corresponding bucket and bunch areas. When the first turn arrives at the start of injection, the voltage required to contain the 2.5 MeV energy spread of the linac beam is 40 kV. The injected beam has a bunch area of 3.3 eV sec, and the waiting bucket has an area of 7.3 eV sec, thus the initial dilution of the area is a factor of 2.2. During injection the voltage is raised to 67 kV to compensate for space charge effects and to give a somewhat larger bucket area. Soon after injection, the bunch is well formed. The bucket area is raised to 9 eV sec, and that area is maintained for the next 7.5 msec. The bucket area beyond that point in time is made larger as indicated in Figure 4 for two reasons. The first is to make the momentum spread of the circulating beam large enough to stay below instability thresholds [5,6], and the second is to provide a synchrotron frequency large enough so that the particles in the bunch can follow the rapidly changing synchronous phase angle near the time of extraction.

### V. IMPEDANCE AND INSTABILITIES

Impedance of the RCS is dominated by space charge which is capacitive for the both longitudinal and transverse components. The RCS operates below the transition energy of the machine, and therefore it is not expected to have longitudinal microwave instability. However a detailed study of longitudinal impedance and instability was performed, and results are presented in this

conference [7]. Similarly, the transverse impedance and instabilities, were analyzed and details are presented in this conference [8].

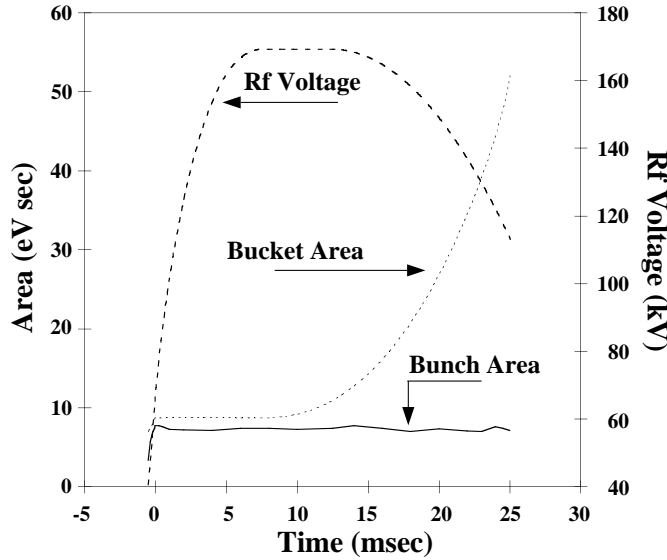


Figure 4: The Rf Voltage Program, Showing Bunch and Bucket Area Over the Complete Cycle.

## VI. SYNCHROTRON HARDWARE

The RCS has ceramic vacuum chambers equipped with rf shields constructed of conducting wires. The system is similar to that used at the ISIS facility at Rutherford-Appleton Laboratory [7].

The RCS ring magnets are energized with dual frequency resonant power supplies that excite the ring at a 20-Hz rate and de-energize it at a 60-Hz rate. This method results in an overall repetition rate of 30 Hz, and reduces the required rf accelerating voltage by 1/3. Detailed descriptions of the hardware can be found in Reference 1.

## VII. SUMMARY

The IPNS Upgrade Feasibility Study resulted in the design of an accelerator system capable of producing 1 MW of proton beam power. The full power can either be delivered to one of the two neutron generating targets, or can be split between them. A scheme of phase-space painting using charge exchange allows injection of 500 turns into the machine. Table 2 is a summary of the main RCS parameters.

Table 2: Main Parameters of the RCS.

Parameters	Values	Units
Circumference	190.4	m
Super-periodicity	4	-
Total number of cells	28	-
Number of normal cells	12	-
Nr. of dispersion suppressor cells	8	-
Nr. of straight section cells	8	-
Nominal straight section length	2.9	m
Injection energy	400	MeV
Injection field	0.463	T
Nominal extraction energy	2.0	GeV

Maximum design energy	2.2	GeV
Dipole field at 2.2 GeV	1.5088	T
Bending radius	6.6207	m
Dipole length	1.3	m
Dipole good field region	0.45	m
Dipole gap height	0.182	m
Number of dipoles	32	-
Number of quadrupoles	56	-
Quadrupole length	0.5	m
Quadrupole aperture radius	0.1185	m
Maximum quadrupole gradient	8.8	T/m
Number of sextupoles (F)	16	-
Number of sextupoles (D)	16	-
Number of harmonic sextupoles	8	-
Maximum sextupole strength	1.2	m <sup>-2</sup>
Sextupole length	0.2	m
Sextupole aperture radius	0.13	m
Horizontal tune, $\nu_x$	6.821	-
Vertical tune, $\nu_y$	5.731	-
Normalized transition energy, $\gamma_t$	5.40	-
Natural chromaticity, $\xi_x = (\Delta v/v)_x/(\Delta p/p)$	-1.06	-
Natural chromaticity, $\xi_y = (\Delta v/v)_y/(\Delta p/p)$	-1.20	-
Maximum $\beta$ function	12	m
Minimum $\beta$ function	2.2	m
Maximum $\eta$ function	2.2	m
Minimum $\eta$ function	-0.06	m
Revolution time at injection	890.1	nsec
Revolution time at extraction	665.1	nsec
$\bullet$	64.5	c
$B_{max}$		T/sec
Maximum energy gain/turn	81.4	keV

## Acknowledgments

We acknowledge D. Haid for help in manipulation of computer graphics and H. Rihel for drawings.

## VIII. REFERENCES

- [1] "IPNS Upgrade - A Feasibility Study", ANL Report ANL-95/13 (April, 1995).
- [2] E. Lessner, Y.-C. Chae, and S. Kim, "Effects of Imperfections on Dynamic Aperture and Closed Orbit of the IPNS Upgrade Synchrotron," in these proceedings.
- [3] Y.-C. Chae and Y. Cho, "Study of Field Ionization in Charge Exchange Injection for the IPNS Upgrade," in these proceedings.
- [4] E. Crosbie and K. Symon, "Injecting a Kapchinskij-Vladimirskij Distribution into a Proton Synchrotron," in these proceedings.
- [5] K. Harkay, Y. Cho, and E. Lessner, "Longitudinal Instability Analysis for the IPNS Upgrade" in these proceedings.
- [6] K. Harkay and Y. Cho, "Transverse Instabilities Analysis for the IPNS Upgrade" these proceedings.
- [7] G. H. Rees, "Status report on ISIS," in Proceedings of the IEEE Particle Accelerator Conference (March 16-19, 1987).